ASIAN JOURNAL OF PHARMACEUTICAL AND CLINICAL RESEARCH

INNOVARE ACADEMIC SCIENCES
Knowledge to Innovation

Vol 18, Issue 8, 2025

Online - 2455-3891
Print - 0974-2441

Research Article

FABRICATION AND CHARACTERIZATION OF CHITOSAN NANOPARTICLES FOR EFFICIENT DELIVERY OF KAEMPFEROL IN BREAST AND CERVICAL CANCER TREATMENT

SARANYA MV, SUDHA T*

Department of Chemistry and Analysis, Vels Institute of Science, Technology and Advance Studies, Pallavaram, Tamil Nadu, India.
***Corresponding author: Sudha T; Email: tsudha.sps@vistas.ac.in**

Received: 15 May 2025, Revised and Accepted: 27 June 2025

ABSTRACT

Objectives: The goal of the present study was to use factorial design to prepare and optimize chitosan nanoparticles loaded with kaempferol for targeted drug delivery. A systematic investigation was conducted into the effects of major preparation variables, polymer amount, sodium tripolyphosphate (TPP) quantity, and stirring speed on drug content, encapsulation efficiency, and cumulative drug release (CDR).

Methods: Using TPP as a cross-linker and chitosan as a biodegradable polymer, kaempferol-loaded chitosan nanoparticles were created through an altered ionic gelation process. The formulation parameters were optimized using a factorial design. A number of nanoparticle characteristics, such as CDR, encapsulation effectiveness, and particle size, were described. A scanning electron microscope was used to investigate the prepared nanoparticles morphology. In addition, the MTT assay was used to evaluate cytotoxicity on the MCF-7 and HeLa human cancer cell line for breast and cervical cancer.

Results: Particle size of 112.5 nm, drug content of 96.63±0.531%, encapsulation efficiency of 89.45±0.311%, cumulative drug release (CDR) of 94.63±0.03%, zeta potential of −24.2 mV, and polydispersity index of 0.192 are all characteristics of the optimal formulation. The nanoparticles' spherical shape was revealed by the scanning electron microscope results. Studies on *in vitro* cytotoxicity revealed that the chitosan nanoparticles loaded with kaempferol demonstrated strong anticancer properties, with IC_{50} values of 68.00 µg/mL for HeLa cell lines and 55.00 µg/mL for MCF-7. The significant p-values were found to be 0.0480, 0.0191, and 0.0372 for all responses. The formulations were included based on chitosan (≥85% deacetylation), kaempferol (≥98% purity), and nanoparticle formulations with size <200 nm, PDI ≤0.3, drug content ≥80%, and encapsulation efficiency ≥70%. Only actively growing, uncontaminated HeLa, and MCF-7 cells (≥95% viability, passages 3–10) were used for cytotoxicity studies.

Conclusion: Therefore, it is possible that the newly discovered nanoparticles for the treatment of breast and cervical cancer represent a ground-breaking approach. These findings significantly support the possibility of using these nanoparticles as a therapeutic treatment for breast and cervical cancer patients undergoing or following resection of malignant lesions.

Keywords: Kaempferol, Chitosan, Nanoparticles, Box–Behnken design, MTT assay.

 DOI: http://dx.doi.org/10.22159/ajpcr.2025v18i8.54428. Journal homepage: https://innovareacademics.in/journals/index.php/ajpcr

INTRODUCTION

A naturally occurring flavonoid, numerous plant sources consist of kaempferol (3,5,7-trihydroxy-2-(4-hydroxyphenyl)-4H-1-benzopyran-4-one). Covering tea, broccoli, apples, grapes, and medicinal herbs. Due to its wide range of pharmacological activities, it has garnered plenty of scientific attention. By scavenging reactive oxygen species and shielding cellular components from oxidative stress-induced damage, studies have shown that kaempferol has strong antioxidant qualities [1].

By inhibiting cytokinesenzymes and pro-inflammatory like, and tumor necrosis factor-alpha, cyclooxygenase-2, and interleukin-6, it also has anti-inflammatory properties [2]. In addition, through mechanisms such as cell cycle arrest, apoptosis induction, and angiogenesis inhibition, kaempferol has demonstrated strong anticancer activity against a range of cancer cell lines, including those from the liver, lung, and colon [3].

Kaempferol is a promising candidate for therapeutic development due to its additional pharmacological actions, which include cardioprotective [4], neuroprotective [5], anti-diabetic [6], antibacterial [7], and hepatoprotective effects [8]. Kaempferol clinical utility is severely limited due to its poor water solubility, low oral bioavailability, and rapid metabolic degradation in the gastrointestinal tract, despite its promising therapeutic potential. Due to these difficulties, an effective drug delivery system that can increase the drug solubility, shield it from deterioration, and offer sustained release is required for increased therapeutic efficacy [9].

Chitosan, a biocompatible and biodegradable natural polysaccharide, has gained significant attention as a promising polymer for nanoparticle-based drug delivery due to its mucoadhesive properties, ability to open tight junctions, and inherent biological activities. Chitosan nanoparticles offer enhanced bioavailability and targeted drug delivery [10]. Alginate chitosan formulations were optimized for pulmonary delivery of D-cycloserine [11]. Antimicrobial and antioxidant activities were also observed in chitosan-based systems [12]. Recent findings highlight their promising anticancer potential [13].

Drug delivery methods based on nanotechnology, especially polymeric nanoparticles, have shown promise in overcoming these constraints. Due to its mucoadhesive, biodegradable, non-toxic, and antimicrobial properties, chitosan [14] a naturally occurring, biodegradable, and biocompatible polysaccharide produced by the deacetylation of chitin is widely used among them. Poorly water-soluble drugs can be encapsulated by chitosan nanoparticles, which also enhance their stability, absorption, and permit the controlled or release of drugs in targeted. Because it is simple to use, organic solvents are avoided, and mild processing conditions that make it appropriate for sensitive bioactives like kaempferol, the ionic gelation technique which uses

chitosan and sodium tripolyphosphate (STPP) as a cross-linking agent is highly preferred [15].

Using a Box–Behnken design (BBD), a kind of response surface methodology that enables systematic evaluation of the effects and interactions of multiple formulation variables with fewer experimental runs, kaempferol-loaded chitosan [16] nanoparticles were developed and optimized for this present study. Drug content, entrapment efficiency (%EE), and particle characteristics were the primary response parameters, whereas the independent variables chosen were chitosan concentration, tripolyphosphate (TPP) concentration, and stirring speed. The formulation was examined and improved for improved performance using the model [17-20].

Zeta potential, shape, particle size, drug loading, entrapment effectiveness, and *in vitro* drug release profile were all additionally examined for the produced nanoparticles. To determine the nanoparticles potential as anticancer agents, their cytotoxic effects will also be evaluated against cervical cancer and breast cancer HeLa, MCF-7 cell lines. This study aims to develop a new and efficient delivery system that could improve the clinical applicability of kaempferol in cancer treatment by combining the medicinal advantages of kaempferol with the beneficial qualities of chitosan nanoparticles.

METHODS

The technique, which was founded on chitosan ionic gelation with anions TPP was modified to create kaempferol-loaded chitosan nanoparticles. A 0.1% v/v water-soluble solution of acetic acid was used to dissolve chitosan (0.2% w/v). A 20% w/v aqueous NaOH solution was used to bring the chitosan solution's pH down to 4.8. Ultrapure water was used to dissolve TPP (0.2% w/v). TPP/chitosan/kaempferol nanoparticles were made using 10 mL of chitosan solution preheated (60° centigrade for 10 min) [21,22].

The solution of kaempferol was added while being magnetically stirred. Subsequently, drop by drop transfers of 3.3 mL of 4°C solution TPP were made to a room-temperature chitosan/kaempferol solution while being stirred magnetically for 30 min. The opalescent suspension developed on its own. After that, the nanoparticle formulation was centrifuged at 12,000 rpm for 30 min and to remove the unencapsulated compounds washed with water. To prevent particle aggregation, the nanoparticle formulation was sonicated for 10 min following centrifugation [23,24].

In vitro evaluation

Particle size and zeta potential (malvern zetasizer)

After being combined with distilled water and sonicated, the chitosan samples loaded with kaempferol were left for half an hour. At 25°C, the analysis was carried out, and at zeta potential, the same process was repeated. To ascertain the stability of the prepared formulations, their zeta potential was described.

Field emission scanning electron microscope (FESEM)

The shape of fractures, surface topography, and texture can all be ascertained using FESEM. The morphology surface of kaempferol-loaded chitosan nanoformulation was determined by a FESEM (Carl Zeiss, supra55, Germany) at the central instrumental facility (Savitribai Phule Pune University). Photographs of samples were taken at a different magnification power (×10,000).

%EE

The %EE of the formulation of kaempferol-loaded nanoparticles was evaluated using the centrifugation method. Ten milligrams of the prepared nanoparticle formulation were placed in an Eppendorf for centrifugation (RM-12) at 1400 rpm for 30 min. The liquid supernatant, which contained the drug that was not entrapped, was then diluted with phosphate buffer pH 6.8 and examined using a ultraviolet (UV) spectrophotometer set to 265 nm. The following formula was used to determine the absorbance %EE using that.

$$\text{Entrapment efficiency in percentage} = \frac{\text{total drug-free drug}}{\text{total drug}}$$

Percentage of CDR

Using a dissolution test apparatus United States Pharmacopeia (USP) type II, a dissolution test was conducted in formulations containing 10 mg of kaempferol and kaempferol-loaded nanoparticles in phosphate buffer pH 6.8. Type-II apparatus USP was used for the dissolution studies, which were carried out at 50 revolutions/min and 37±0.5° centigrade. 900 mL of dissolution media were contained in the dissolution apparatus and filled with 10 mg of the medication. At intervals of 10, 20, 30, 40, 50, 60, 90, and 120 min, the 5 mL solution was removed, and the beaker was filled with an equivalent volume of phosphate buffer solution. UV-visible spectroscopy at 265 nm was used to measure the drug's dissolved amount.

Drug content

The weighed amount of 10 mg kaempferol-loaded chitosan nanoparticles was collected in standard flask of 10 mL, and the volume was made up with methanol and sonicated for 15 min. After that, 1 mL of this mixture was diluted to 10 mL with methanol, and the percentage drug content was observed at 265 nm using a UV spectrophotometer (Jasco V-630). The drug content was calculated using the calibration curve method.

Stability studies

For 90 days (3 months), the chitosan nanoparticles loaded with kaempferol were stored at a comfortable temperature (25°C) and in a fridge (2–8°C). Drug content, drug release percentage, and %EE were calculated.

Cytotoxicity assay

The MCF-7 and HeLa cancer cells were cultivated in fetal bovine serum (10%) in electronics and mechanical engineer medium National Centre for Cell Science, Pune were produces the cancer cells. The cells were maintained at air 95%, 37.0° centigrade, and humidity 100%. Upkeep the culture medium was changed twice a week, and cultures were passed once a week.

Cell therapy procedure

Single cells are utilized for producing single-cell suspensions by trypsin-ethylenediaminetetraacetic acid. To reach a final density of 1×10^5 cells/mL, viable cells were diluted with medium containing 5%. Fetal bovine serum after being counted using a hemocytometer. At a plating density 10,000 cells/well, 100 µL of cell suspension were added to each well of 96-well plates. The plates had been incubating at 37.0° centigrade, 5% carbon dioxide, 95% air, and 100% humidity to permit for linking of cells. The test samples serial concentrations were applied to the cells after a 24 h period.

After being dissolved in clean dimethyl sulfoxide (DMSO), serum free medium had been utilized to dilute a small amount of the sample solution to double the intended greatest maximum concentration in the test. Four different serial dilutions were created.

Four additional serial dilutions were made to obtain five concentrations of the samples. One hundred microliter small amounts of each of these different sample dilutions were added to the corresponding wells that already contained 100 µL of medium to achieve the needed concentrations of the final sample.

For a further 48 h, the plates were set aside at 37.0° centigrade, 5% carbon dioxide, air 95%, and 100% humidity after the sample was added. For every concentration, triplicate was maintained, and the medium devoid of samples was used as the control.

MTT assay

Water-soluble yellow tetrazolium salt is known as MTT. The mitochondrial enzyme succinate dehydrogenase that exists in cells that live splits the tetrazolium band, modifying the MTT into an inert pink formaldehyde. Thus, the volume of formaldehyde generated is instantly to the quantity of living cells. Following 48 h of growth, 15.0 µL of MTT (5.0 mg/mL) in phosphate buffered saline had been inserted into every hole, the holes then underwent incubation for 4 h at 37.0° centigrade. Following the MTT's shut down containing medium, the formed crystals of formazan were disbanded in 100 µL of DMSO, and evaluations have been taken through a reader with a microplate the absorbance at 570 nm.

Then, the percentage of cell viability was calculated using the formula below compared to control:

$$\text{Percentageviabilit of cell} \quad \frac{\text{Absorbance of test}}{\text{Absorbance of contro}} \times 100$$

The percentage of cell inhibition was computed using the following formula.

Inhibition percentage of cell = 100 - % viability of cell

GraphPad Prism software was used to calculate the IC_{50} and plot a graph of nonlinear regression between the log concentration and the % of cell inhibition.

RESULTS AND DISCUSSION

Experimental design

The positive results of kaempferol-loaded chitosan nanoparticles formulations were described in this research study. Chitosan (mg) (A), STPP (B), and stirring speed (C) were acknowledged as the most critical variables affecting the drug content, encapsulation efficiency%, and *in vitro* drug release through the initial trials. In the existing design methods, the BBD is rotatable or almost rotational, has minute collinearity, and has good design qualities. Other methods might have orthogonal blocks or be insensitive to absent data. They struggle to anticipate at the edges of the design space as a result of them. BBD works well for structuring second-order polynomial models and identifying quadratic response surfaces. It is made up of a collection of virtual center points that lie at the middle of each multi-dimensional cube boundary. According to BBD, 13 runs were indispensable for the response surface approach. The factor permutations which gave different responses are illustrated in Table 1. Obviously, every variable of dependence depends on the variables that are not dependent that were chosen. This can be calculated from a wide range of the 13 runs. Design-Expert-Stat-Ease software (13.0 Version) was used to analyze the data to obtain regression equations, regression coefficients, and analysis of variance (ANOVA).

Kaempferol-loaded chitosan nanoparticles have the drug content percentage between 88.36 and 96.63%. The model's F-value of 9.07 showed that it was significant, and the particle size factorial equation showed a good correlation coefficient 1.000. Model terms were considered valuable when the prob>F values were <0.0480. Among these chitosan concentration (A), stirring speed (C), and the quadratic term of STPP (B^2) were identified as significant factors affecting drug content. In contrast to the pure error, the lack of fit was substantial, as indicated by the lack of fit f-value of 9.07. A large lack of fit f-value was 4.80% likely to be the result of noise. The reports are shown in Table 2.

Chitosan concentration (A) has a considerable impact on drug content, both directly and through its interaction with stirring speed (C), according to the ANOVA results. This suggests that the combination of these two factors has a significant impact on the efficiency of drug content. The influence of chitosan on drug content varies according to the stirring speed used during formulation, as seen by the notably high interaction between chitosan and stirring speed (AC) (p=0.0161). Its quadratic term (B^2) was significant (p=0.0379), suggesting a non-linear relationship where intermediate levels of STPP may be more advantageous for drug content than very low or high levels, even when STPP (B) does not have a significant individual or interaction effect.

The drug content, the precise amount of drug in the finished formulation was influenced by both the chitosan concentration and the speed at which it was stirred. By creating a more durable matrix that holds more drug during the production of nanoparticles, chitosan concentration may initially improve drug integration. Beyond a certain point, though, too much chitosan can cause uneven drug distribution and increased viscosity, which could reduce the total amount of medicine. The speed at which the drug was stirred affects how evenly it disperses throughout the chitosan matrix. Better mixing at moderate speeds enhances drug content by enabling more consistent drug loading. A speed that is too high may cause mechanical degradation or drug expulsion from the matrix, while a speed that is too low may cause drug loss or uneven distribution due to insufficient mixing. Because chitosan and stirring speed (AC) have a substantial interaction, the effect of one depends on the degree of the other, only when both are properly balanced can the drug content be at its best. The predicted versus actual plot Fig. 1a shown compares the experimentally observed drug content values with the values predicted by the statistical model. The contour plot Fig. 1b illustrates the combined effect of chitosan (A) and STPP (B) on drug content (%) at a fixed stirring speed of 750 rpm. The three dimension response surface plots in Fig. 1c were used to illustrate the impact of the primary and interactive effects of independent variables on the drug content.

Table 1: DOE (BBD) suggested experimental batches

Run	Factor-1 Chitosan (mg)	Factor-2 sodium tripoly phosphate (mL)	Factor-3 stirring speed (RPM)	Drug content (%) (R1)	Entrapment efficiency (%) (R2)	Cumlative drug release (%) (R3)
1	110	3	750	91.34	88.2	89.16
2	65	3.3	500	91.25	85.52	89.19
3	65	3.15	750	91.36	84.69	89.78
4	20	3.15	1000	90.31	85.47	88.19
5	65	3	500	88.36	84.8	85.19
6	20	3.3	750	89.37	87.35	87.69
7	20	3.15	500	92.56	84.21	89.78
8	110	3.3	750	90.47	83.86	88.17
9	110	3.15	500	91.36	84.65	90.20
10	110	3.15	1000	96.63	89.45	94.63
11	65	3	1000	91.05	88.01	88.19
12	65	3.3	1000	91.21	86.12	86.17
13	20	3	750	88.85	84.8	85.14

%: Percentage, R1: Response 1, R2: Response 2, R3: Response 3. BBD: Box-Behnken design

Table 2: Quadratic model for response drug content (R1) ANOVA findings

The source	SS	Degrees of freedom	MS	Fit value	Prob. value	Findings
Model	47.77	9	5.31	9.07	0.0480	Significant
A-Chitosan	9.48	1	9.48	16.21	0.0275	
B-Sodium tripolyphosphate	0.9112	1	0.9112	1.56	0.3005	
C-Stirring speed	4.02	1	4.02	6.87	0.0789	
AB	0.4830	1	0.4830	0.8258	0.4305	
AC	14.14	1	14.14	24.17	0.0161	
BC	1.86	1	1.86	3.19	0.1723	
A^2	0.4577	1	0.4577	0.7826	0.4415	
B^2	7.41	1	7.41	12.66	0.0379	
C^2	1.88	1	1.88	3.22	0.1707	
Residual	1.75	3	0.5849			
Cor total	49.52	12				

SS: Sum of square, MS: Mean square, ANOVA: Analysis of variance

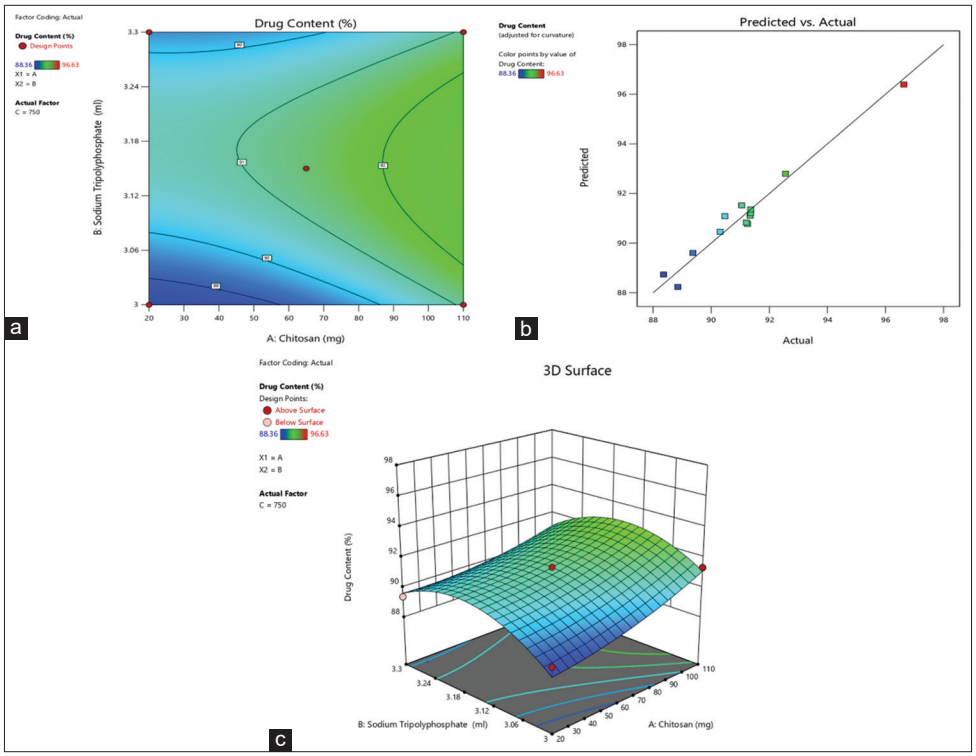

Fig. 1: (a) Plot contour for drug content (%), (b) predicted versus actual plot, predicted versus actual plot for drug content (%), and (c) 3D response surface plot, 3D response surface plot for drug content (%)

The mathematical model made for encapsulation efficiency % (R2) was observed to be substantial with fit-value of 6.52 (prob <0.0191) and R squared value of 0.8671. The independent variables are A, B, and C, including the quadratic term. The model is significant as p<0.0191. This was revealed in Table 3. The relevance of the lack of fit is indicated by the lack of fit value of 6.52. A large lack of fit value was 1.91% likely to be brought on by noise. For the model to F, there ought to be a notable absence of F. Notable not being suitable is good for the model to suitable. Outcomes of the equation imply that the effects of C and AB are more important. Among the individual terms, stirring speed (C) shows a highly significant impact (p=0.0086), suggesting it plays a critical role in enhancing %EE, possibly due to its influence on particle formation and encapsulation dynamics. The interaction between chitosan and STPP (AB) is also significant (p=0.0091), indicating a synergistic effect between these two components on the efficiency. Stirring speed significantly affects %EE because it directly influences the size, uniformity, and stability of the nanoparticles or microcapsules formed during the encapsulation process. In contrast, chitosan (A), STPP (B), and the remaining interaction terms (AC and BC) are not statistically significant (p>0.05), implying their individual or combined effects are relatively minor or inconsistent within the studied range. Overall, optimizing stirring speed and the AB interaction was key for maximizing %EE. The contour plot, predicted versus actual plot, and three-dimensions response surface plot (Fig. 2a-c) demonstrated the primary effects of C, B, and A on the encapsulation efficiency (R2) of kaempferol-loaded chitosan nanoparticles. The encapsulation efficiency increases from 83.86% to 89.45% at high levels of C. The ANOVA findings for %EE reports are shown in Table 3.

The precise model made for CDR (R3) was discovered to be substantial with fit value of 10.92 (prob <0.0001) and R squared value of 0.9704. A, B, and C which are the independent variables have significant effects on the CDR. The F-value of 6.52 suggests that a lack of fit was significant. The chances that noise could be the cause of such a large lack of fit F-value was 3.72%.

The model was significant as the Prob values below 0.0500 are considered significant. In this model, the terms A, B^2 (the quadratic

Table 3: Response entrapment efficiency with a quadratic model (R_2) ANOVA findings

The source	SS	Degree of freedom	MS	Fit value	Prob. value	Findings
Model	32.32	6	5.39	6.52	0.0191	Significant
A-Chitosan	2.34	1	2.34	2.84	0.1430	
B-Sodium tripolyphosphate	1.10	1	1.10	1.33	0.2933	
C-Stirring speed	12.18	1	12.18	14.75	0.0086	
AB	11.87	1	11.87	14.37	0.0091	
AC	3.13	1	3.13	3.79	0.0994	
BC	1.70	1	1.70	2.06	0.2010	
A^2	2.43	1	2.43	3.61	0.1431	
B^2	21.02	1	21.02	25.23	0.0243	
C^2	0.1010	1	0.1010	0.1253	0.5317	
Residual	4.96	6	0.8258			
Cor total	37.27	12				

SS: Sum of square, MS: Mean square, ANOVA: Analysis of variance

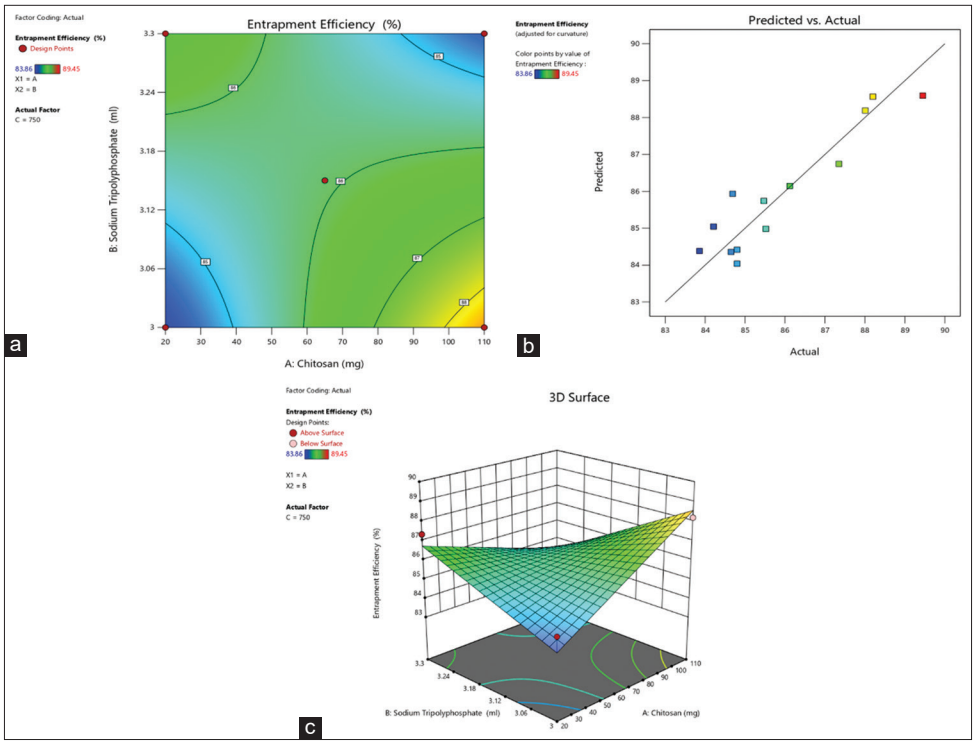

Fig. 2: (a) Plot contour for entrapment efficiency (%), (b) predicted versus actual plot for entrapment efficiency (%), and (c) 3D response surface plot for entrapment efficiency (%)

term of B), and the interaction term AC were found to be statistically significant. Among the individual factors, chitosan (A) has a strong and significant influence (p=0.0213), suggesting its concentration plays a critical role in determining the outcome, likely due to its impact on matrix formation or interaction with the drug. The AC interaction (between chitosan and stirring speed) was also significant (p=0.0449), highlighting that their combined effect meaningfully alters the response, possibly through influencing particle formation or entrapment dynamics. Although stirring speed (C) shows a borderline effect (p=0.0762), it may still be important in fine-tuning the formulation. The quadratic term B^2 is highly significant (p=0.0110), indicating a non-linear effect of STPP, where moderate levels may be more effective than very high or low concentrations. The major consequences of A, B, and C on the percentage CDR (R3) of kaempferol-loaded chitosan nanoparticles are illustrated Table 4. The contour plot, and three-dimension response surface plot (Fig. 3a-c) were illustrated main influences of C, B, and A on the % CDR (R3) of kaempferol-loaded chitosan nanoparticles.

Squared is the coefficient of determination. Since it is a ration of the fraction of the total squared error, the value of R^2 ranges from 0 to 1. It is better if the value is closer to one. Nevertheless, a large value of R^2 does not certainly denote a good regression model. Adding a variable to the model will always increase, regardless of the statistical significance of the additional variable, R^2 will be increased if available is added into the model. The adjusted R-squared statistic is crucial in which its value falls if pointless variables are incorporated. The regression equation for all responses is shown in Table 5.

The existence of extraneous term scan be implied when the two statistics are used together in the computed model which a large difference between the values of R^2 and Adj-R^2 is >0.2. Residual is the difference in the amount of estimated output and the real output. PRESS is a measurement of the extent of the model suits individual aspect in the design. Predicted R^2 can be calculated by PRESS. Adeq precision is applied to measure the signal to noise ratio. Preferably, the ratio should be more than four. The adequate precision values for R1 (12.1633), R2 (6.8288), and R3 (12.0763) indicate that each model has an adequate

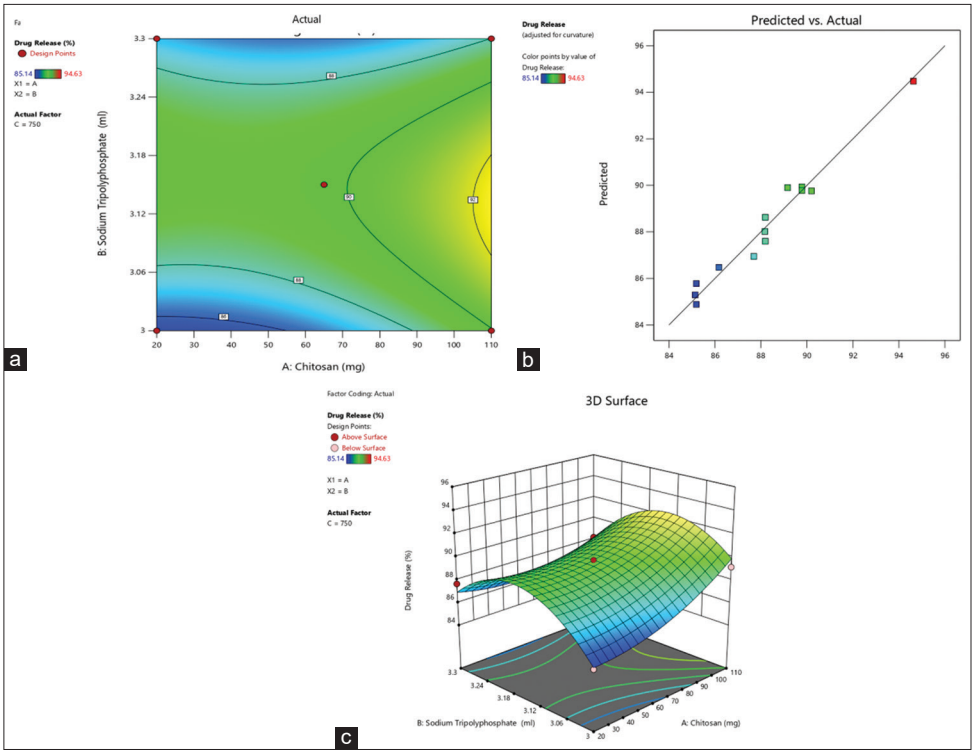

Fig. 3: (a) Plot contour for cumulative drug release (%), (b) predicted versus actual plot for cumulative drug release (%), and (c) 3D response surface plot for cumulative drug release (%)

Table 4: Quadratic model for response cumulative drug release (R_3) ANOVA findings

The source	SS	Degree of freedom	MS	Fit value	Prob value	Findings
Model	80.60	9	8.96	10.92	0.0372	Significant
A-Chitosan	16.13	1	16.13	19.67	0.0213	
B-Sodium tripolyphosphate	0.0265	1	0.0265	0.0322	0.8689	
C-Stirring speed	5.81	1	5.81	7.09	0.0762	
AB	3.13	1	3.13	3.82	0.1457	
AC	9.06	1	9.06	11.05	0.0449	
BC	1.02	1	1.02	1.24	0.3461	
A^2	2.96	1	2.96	3.61	0.1538	
B^2	26.07	1	26.07	31.79	0.0110	
C^2	0.1081	1	0.1081	0.1318	0.7406	
Residual	2.46	3	0.8202			
Cor total	83.07	12				

SS: Sum of square, MS: Mean square, ANOVA: Analysis of variance

Table 5: Regression equation for the responses

Response regression equation
R1=+91.36+1.09A+0.3375B+0.7087C-0.3475AB+1.88AC−0.6825BC +0.4475$A^2$0−1.80B^2+0.9075C^2
R2=+85.93+0.5412A−0.3700B+1.23C−1.72AB+0.8850AC−0.6525BC +0.4363A^2−2.50B^2+0.6510C^{-2}
R3=+89.78+1.42A−0.0575B+0.8525C−0.8850AB+1.50AC−0.5050BC +1.14A^2−3.38B^2−0.2175C^2

R1: Drug content, R2: Entrapment efficiency, R3: Cumulative drug release

Table 6: ANOVA-obtained statistical parameters and reduced response surface models

Interactions	R^2	Adjusted R^2	Predicted R^2	Adeq precision
R1	0.9646	0.8583	0.8435	12.1633
R2	0.8671	0.7341	0.4403	6.8288
R3	0.9704	0.8815	0.8875	12.0763

R^2, Adjusted R^2, Predicted R^2 and adequate precision-analysis of variance values

signal and can be used to navigate the design space. The design space can be navigated with the help of this model. These statistics are employed with an intention of avoiding over suiting of model. ANOVA derived statistical parameters and reduced response surface models are shown in Table 6.

The CF10 batch code of kaempferol-loaded chitosan nanoparticles formulated following the construction of the polynomial equations connecting the dependent and independent variables, in accordance with the optimized levels. By placing restrictions on the dependent and independent variables, the optimization conditions were obtained. The observed values closely matched the optimized process expected values. The CF10 formulation % drug content, efficiency entrapment %, and drug release cumulative % have been found to be 96.63±0.531, 89.45±0.311%, and 94.63±0.03.

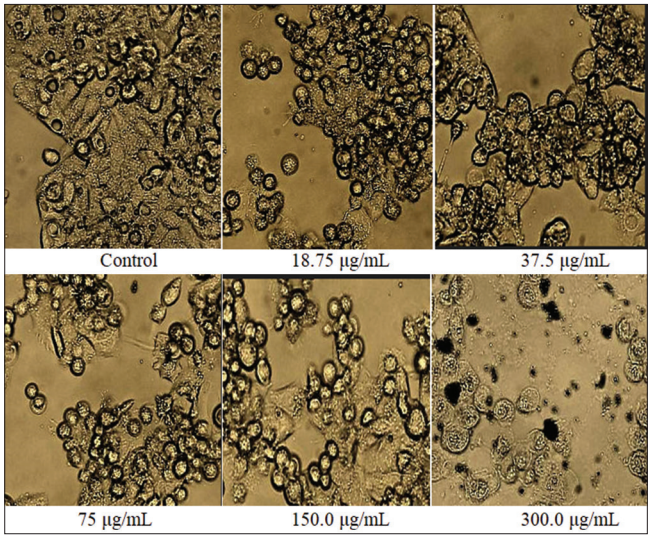

Fig. 4: Cytotoxicity images for cell line MCF-7 for breast cancer study

The CF10 formulation demonstrates favorable characteristics in terms of size of the particle, polydispersity index, and zeta potential. The size of the particle of 112.5 nm suggests that the formulation is within an optimal range for drug delivery, ensuring efficient absorption and stability. The polydispersity index value of 0.192 indicated a narrow distribution of particle sizes, which is ideal for formulation uniformity. In addition, the zeta potential of −24.2 mV reflects good colloidal stability, as the negative charge helps prevent aggregation of nanoparticles. These properties suggest that CF10 was a promising formulation with suitable characteristics for effective drug delivery applications.

The targeted inhibitory effects on the MCF-7 breast cancer cell line using chitosan nanoparticles loaded with kaempferol at different concentrations ranging from 18.75 µg/mL to 300 µg/mL, with an untreated control for comparison the microscopic images that were provided. A dense, healthy monolayer of MCF-7 cells with tight adherence and normal morphology can be seen in the control image. Progressive morphological deterioration is visible as the nanoparticle concentration rises. There is a slight disruption and less cell clustering at 18.75 µg/mL and 37.5 µg/mL. More noticeable cytotoxic effects, such as cell rounding, detachment, and a drop in cell density, express at 75.0 µg/mL and 150.0 µg/mL. Cytotoxicity images for MCF -7 cell line for breast cancer study are shown in Fig 4.

The most significant changes occur at 300.0 µg/mL, where cellular debris, fragmentation, and a notable loss of viable cells signify widespread cell death. These results bolster the possibility of kaempferol-loaded chitosan nanoparticles as an agent approach in the treatment of breast cancer by showing a dose-dependent cytotoxic response congruent with the IC_{50} value of 55.12 µg/mL. Percentage inhibition findings for MCF-7 cell line for breast cancer study are shown in Table 7.

The images illustrate the cytotoxic impacts of varying concentrations of chitosan nanoparticles carrying kaempferol on HeLa cervical cancer cell lines in comparison with an untreated control (18.75–300.0 µg/mL). HeLa cells in the control group are tightly packed, adherent, and morphologically intact, indicating normal growth. Early indicators of cytotoxicity, including mild cell rounding and a loosening of intercellular attachments, are seen at 18.75 µg/mL and 37.5 µg/mL. Cellular shrinkage, detachment, and decreased confluency are among the more noticeable morphological changes seen in the images as concentrations rise, particularly at 75.0 µg/mL and 150.0 µg/mL. At maximum concentration, there was a notable reduction in the amount of viable cells, alongside extensive cellular death and disintegration, revealing

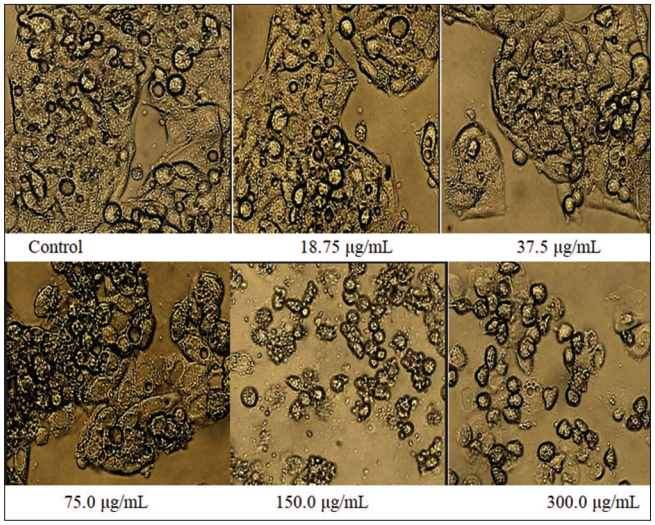

Fig. 5: Cytotoxicity images for HeLa cell line for cervical cancer study

Table 7: Percentage inhibition reports for cell line MCF-7 for breast cancer study

Conc (µg/mL)	Average absorbance	% inhibition	IC_{50} value
18.75	0.5250±0.341	17.32	55.12 µg/mL
37.5	0.3872±0.565	39.06	
75.0	0.2726±0.732	57.16	
150.0	0.2023±0.601	68.18	
300.0	0.1173±0.813	81.57	
Control	0.6353±0.473		

n=3, mean±standard deviation, %inhibition: Percentage inhibition, IC_{50}: Inhibitory concentration

Table 8: Percentage inhibition reports for HeLa cell line for cervical cancer study

Conc (µg/mL)	Average absorbance	% inhibition	IC_{50} value
18.75	0.4193±0.673	16.86	68.00 µg/mL
37.5	0.3336±0.455	33.92	
75.0	0.2336±0.760	53.76	
150.0	0.1446±0.479	71.42	
300.0	0.0753±0.805	85.11	
Control	0.5046±0.645		

n=3, mean±standard deviation, % inhibition: Percentage inhibition, IC_{50}: Inhibitory concentration

widespread cell destruction and cell fragmentation (300.0 µg/mL). This dose-dependent pattern of cytotoxicity indicates that chitosan nanoparticles loaded with kaempferol are capable of effectively causing HeLa cell death, thereby bolstering their ability to serve as an agent for the treatment of cancer cervical. Cytotoxicity images for HeLa cell line for cervical cancer study are shown in Fig 5.

The concentration at which 50% of the cell population is inhibited or rendered non-viable was indicated by the IC_{50} value of 68.00 µg/mL for the chitosan nanoparticles loaded with kaempferol against HeLa cervical cancer cells. This figure illustrates the nanoparticle formulation moderate ability to cytotoxicity affect cervical cancer cells. Cell rounding, membrane blebbing, detachment, and decreased cell density are examples of dose-dependent morphological changes seen in the microscopic images that correlate with this IC_{50} concentration, becoming especially noticeable around and above 68.00 µg/mL. The IC_{50} is a crucial metric for assessing the formulation anticancer efficacy, indicating that kaempferol can significantly inhibit HeLa cell proliferation when it is efficiently used through chitosan nanoparticles.

This finding bolsters the therapeutic potential of kaempferol delivery through nanoparticles for the treatment of cervical cancer. Percentage inhibition reports for HeLa cell line for cervical cancer study are shown in Table 8 [25-27].

CONCLUSION

Optimization and validation of kaempferol-loaded chitosan nanoparticles using BBD were an effective way of optimizing the formulation parameters for obtaining maximum %EE of the drug, controlled release, and suitable nanoparticle attributes. Statistical modeling established the effectiveness of variables such as chitosan concentration, STPP, and stirring rate in affecting main response results such as drug content and %EE. The nanoparticles had favorable physicochemical characteristics, such as ideal particle size, surface charge (zeta potential), and morphology, which are crucial for improved stability and cellular uptake. *In vitro* tests against MCF-7 and HeLa cell lines showed significant anticancer activity as estimated by the measured IC_{50} of 55.12 µg/mL for MCF-7 and 68.00 µg/mL for HeLa, indicating that cytotoxicity increases with higher concentration levels of the sample.

These results emphasize the potential of chitosan as a biocompatible and biodegradable polymer for efficient delivery of poorly soluble phytochemicals such as kaempferol. In general, the research emphasizes the potential of this nanoformulation as a safe, efficient, and targeted drug delivery system that can be further investigated in preclinical and clinical environments for cancer therapeutics.

ACKNOWLEDGMENT

The provided research facilities and the encouragement given in completing the novel Vels Institute of Science and Technology and Advanced Studies, Pallavaram, Chennai, Tamilnadu, deserves a gratitude from the authors.

AUTHOR'S CONTRIBUTIONS

Concept- T.S., M.V.S.; Design-S.T.; Supervision- T.S., M.V.S.; Resources- T.S., M.V.S.; Materials- T.S., M.V.S.; Data collection and/or processing- T.S., Analysis and/or Interpretation- T.S., M.V.S.; Literature Search- T.S., Writing – T.S., M.V.S.; and Critical Reviews- T.S., M.V.S.

CONFLICTS OF INTEREST STATEMENT

No conflicts of interest were disclosed by the authors.

REFERENCES

1. Hosseini A, Alipour A, Baradaran Rahimi V, Askari VR. A comprehensive and mechanistic review on protective effects of kaempferol against natural and chemical toxins: role of NF-κB inhibition and Nrf2 activation. BioFactors. 2023;49(2):322-50. doi: 10.1002/biof.1923, PMID 36471898
2. Wang X, Zhao Y, Liu L, Li J, Li X. Anti-inflammatory mechanisms of kaempferol in chronic diseases. Int Immunopharmacol. 2023;113:109417. doi: 10.1016/j.intimp.2023.109417
3. Kumar S, Kaempferol PA. A dietary flavonoid with promising anticancer properties. Pharmacol Res. 2023;190:106682. doi: 10.1016/j.phrs.2023.106682
4. Kamisah Y, Jalil J, Yunos NM, Zainalabidin S. Cardioprotective properties of kaempferol: A review. Plants (Basel). 2023;12(11):2096. doi: 10.3390/plants12112096, PMID 37299076
5. Zhang W, Liu Q, Zhao M, Xu L, Huang R. Neuroprotective effects of kaempferol in models of neurodegenerative diseases. Neurochem Int. 2023;160:105420. doi: 10.1016/j.neuint.2023.105420
6. Singh D, Patel M, Rana A. Kaempferol as a potential therapeutic agent for diabetes management. J Ethnopharmacol. 2023;310:116345. doi: 10.1016/j.jep.2023.116345
7. Xu Y, Zhang J, Zhang R, Hu X, Lu X. *In vitro* antibacterial activity of kaempferol and its synergistic effect with colistin against colistin-resistant Gram-negative bacteria. J Appl Microbiol. 2021;131(3):1158-70. doi: 10.1111/jam.14991
8. Tang SM, Deng XT, Zhou J, Li QP, Ge XX, Miao L. Pharmacological basis and new insights of quercetin action in respect to its anti-cancer effects. Biomed Pharmacother. 2020;121:109604. doi: 10.1016/j.biopha.2019.109604, PMID 31733570
9. Imran M, Salehi B, Sharifi-Rad J, Aslam Gondal T, Saeed F, Imran A, *et al*. Kaempferol: A key emphasis to its anticancer potential. Molecules. 2019;24(12):2277. doi: 10.3390/molecules24122277, PMID 31248102
10. Srinivas Murthy BR, Yelavarthi PR, Devanna N. Process of orlistat-loaded chitosan nanoparticles using Box-Behnken design - an evaluation study. Asian J Pharm Clin Res. 2021;14(5):103-11. doi: 10.22159/ajpcr.2021.v14i5.41441
11. Jomy S, Muddasir S. Formulation, optimization, and characterization of biocompatible inhalable D-cycloserine-loaded alginate-chitosan nanoparticles for pulmonary drug delivery. Asian J Pharm Clin Res. 2016;9 Suppl 2:82-95.
12. Jacob V, Rajiv P. *In vitro* analysis: The antimicrobial and antioxidant activity of zinc oxide nanoparticles from *Curcuma longa*. Asian J Pharm Clin Res. 2019;12(1):200-4. doi: 10.22159/ajpcr.2019.v12i1.28808
13. Wikantyasning ER, Mazidah Z, Da'i M, Kusumawati IT, Suprapto S. Anticancer studies of zerumbone-loaded chitosan-oleic acid nanoparticles against T47D breast cancer cells. Int J App Pharm. 2024;16(6):66-71. doi: 10.22159/ijap.2024.v16s6.TY2036
14. Gomes AS, Simplicio SS, Gonsalves JK. Chitosan nanoparticles as a potential drug delivery system in the skin: A systematic review based on *in vivo* studies. Chem Select. 2024;9:e202402058. doi: 10.1002/slct.202402058
15. Radhakrishnan J, Suma S, Nair AS, Ramachandran R. Curcumin-loaded chitosan-coated 5-fluorouracil encapsulated nanozeolitic imidazolate framework for combination cancer therapy. J Pharm Innov. 2023;18:2043-53. doi: 10.1007/s12247-023-09770-1
16. Sangnim T, Dheer D, Jangra N, Huanbutta K, Puri V, Sharma A. Chitosan in oral drug delivery formulations: A review. Pharmaceutics. 2023;15(9):2361. doi: 10.3390/pharmaceutics15092361
17. Liu X, Zhang H, Chen Y, Xu L, Yang S, Feng Y. Kaempferol role in modulating oxidative stress in metabolic disorders. Free Radic Biol Med. 2023;193:123-32. doi: 10.1016/j.freeradbiomed.2023.01.012
18. Zhou Y, Zhang X, Wang L, Chen J, Liu Y, Huang Q, *et al*. Kaempferol inhibits cancer cell proliferation by targeting the PI3K/Akt pathway. Mol Cancer Ther. 2023;22(1):45-55. doi: 10.1158/1535-7163.MCT-22-0456
19. Zhang L, Huang Q, Li Y. Kaempferol attenuates liver fibrosis via TGF-β1/Smad signaling pathway inhibition. Phytol Med. 2023;115:154789. doi: 10.1016/j.phymed.2023.154789
20. Gao Y, Zhang T, Li M. Kaempferol suppresses tumor angiogenesis by down regulating VEGF expression. Cancer Lett. 2023;560:215-23. doi: 10.1016/j.canlet.2023.01.012
21. Mehta A, Hanini A, Shah A, Bhatt P, Pathak Y. Advancements in chitosan-based nanoparticles for targeted drug delivery. Carbohydr Poly. 2023;301:120123. doi: 10.1016/j.carbpol.2023.120123
22. Verma S, Gupta M, Sharma P, Mishra V, Jain K. Chitosan nanoparticles: A versatile platform for drug delivery. J Control Release. 2023;355:123-36. doi: 10.1016/j.jconrel.2023.01.045
23. Chen X, Liu J, Zhang Q, Xu T, Huang Y. Chitosan-based nanocarriers for cancer therapy: Recent advances and challenges. Colloids Surf B Biointerfaces. 2023;218:112743.
24. Chen L, Huang M, Zhao Q, Feng Y, Li T. Chitosan nanoparticles for mucosal drug delivery. Inter Pharma. 2023;628:122345. doi: 10.1016/j.ijpharm.2023.122345
25. Li Q, Zhang W, Huang R, Zhao M, Feng L, Xu T, Yang L. Chitosan nanoparticles in cancer therapy: A review. J Biomed Mater Res A. 2023;111(3):567-78. doi: 10.1002/jbm.a.37480
26. Verma R, Kumar A, Patel M, Joshi R, Chauhan D. Kaempferol-loaded chitosan nanoparticles: A promising strategy for cancer therapy. J Drug Deliv Sci Technol. 2023;81:104123. doi: 10.1016/j.jddst.2022.104123
27. Kumar V, Patel A, Joshi M, Chauhan R, Gupta P. Kaempferol-loaded chitosan nanoparticles: Formulation, characterization and *in vitro* evaluation for cancer treatment. J Mol Liq. 2023;384:122003. doi: 10.1016/j.molliq.2023.122003